Asymmetry is defined during meiosis in the oocyte of the parthenogenetic nematode Diploscapter pachys

Dureen Samandar Eweis, Marie Delattre, Julie Plastino

Developmental Biology 483 (2022) 13–21

Contents lists available at ScienceDirect

Developmental Biology

journal homepage: www.elsevier.com/locate/developmentalbiology

Asymmetry is defined during meiosis in the oocyte of the parthenogenetic nematode *Diploscapter pachys*

Dureen Samandar Eweis [a], Marie Delattre [b], Julie Plastino [a,1,*]

[a] Physico Chimie Curie, Institut Curie, Université PSL, CNRS, Sorbonne Université, 75005, Paris, France
[b] Laboratory of Biology and Modeling of the Cell, Ecole Normale Supérieure de Lyon, CNRS, Inserm, UCBL, 69007, Lyon, France

ARTICLE INFO

Keywords:
Asymmetric cell division
Actin
Symmetry breaking
Polarity
Parthenogenesis
Microtubule aster

ABSTRACT

Asymmetric cell division is an essential feature of normal development and certain pathologies. The process and its regulation have been studied extensively in the *Caenorhabditis elegans* embryo, particularly how symmetry of the actomyosin cortical cytoskeleton is broken by a sperm-derived signal at fertilization, upstream of polarity establishment. *Diploscapter pachys* is the closest parthenogenetic relative to *C. elegans*, and *D. pachys* one-cell embryos also divide asymmetrically. However how polarity is triggered in the absence of sperm remains unknown. In post-meiotic embryos, we find that the nucleus inhabits principally one embryo hemisphere, the future posterior pole. When forced to one pole by centrifugation, the nucleus returns to its preferred pole, although poles appear identical as concerns cortical ruffling and actin cytoskeleton. The location of the meiotic spindle also correlates with the future posterior pole and slight actin enrichment is observed at that pole in some early embryos along with microtubule structures emanating from the meiotic spindle. Polarized location of the nucleus is not observed in pre-meiotic *D. pachys* oocytes. All together our results are consistent with the idea that polarity of the *D. pachys* embryo is attained during meiosis, seemingly based on the location of the meiotic spindle, by a mechanism that may be present but suppressed in *C. elegans*.

1. Introduction

Asymmetric cell division produces daughter cells of different fate and usually of different size, and as such, it promotes cellular diversity. The mechanisms ensuring asymmetric cell division have been studied and understood using a relatively limited range of model systems, including the first cell division of the *Caenorhabditis elegans* embryo (Gönczy, 2008; Knoblich, 2010).

C. elegans embryos are arrested at prophase of meiosis I until fertilization. Upon sperm entry and towards the end of meiosis II, the network of actin and myosin that underlies the embryo membrane, known as the cortex, begins contracting all around the embryo (Munro et al., 2004). The discrimination of one pole of the embryo from the other, or symmetry breaking, is a fundamental prerequisite for asymmetric cell division (Gan and Motegi, 2021). In the fertilized *C. elegans* embryo, symmetry breaking has been shown to depend on a sperm centrosome-derived kinase AIR-1 (Kapoor and Kotak, 2019; Klinkert et al., 2019; Zhao et al., 2019). This kinase locally weakens the actomyosin cortex, triggering a contraction away from the sperm centrosome at the presumptive posterior pole. This produces directed cytoplasmic streaming and anterior-directed actomyosin cortical flows, which are accompanied by intense cortical ruffling and a traveling deep invagination, known as the pseudocleavage furrow that separates a smooth posterior cortex from a dynamic anterior cortex (Hird and White, 1993; Munro et al., 2004). As a result of actomyosin symmetry breaking, an actin-rich anterior domain is formed and the PAR polarity proteins are segregated differentially with anterior localization of PAR-3, PAR-6, and PKC-3 while PAR-1 and PAR-2 are recruited to the posterior cortex (Munro et al., 2004). During cortical polarity establishment, the maternal and paternal pronuclei meet at the posterior pole, and migrate to the cell center in a microtubule-dependent manner. During anaphase, the mitotic spindle is subsequently off-centered as a result of an imbalance of microtubule pulling forces from the anterior versus the posterior cortex, resulting in unequally-sized daughter cells (Rose and Gönczy, 2014).

Despite sometimes vast evolutionary distances, a conserved feature of nematodes studied so far is embryo polarization as early as the first cell division (Brauchle et al., 2009; Schulze and Schierenberg, 2011; Valfort et al., 2018). The manifestation of this early polarization is as follows: i)

* Corresponding author.,
E-mail address: julie.plastino@phys.ens.fr (J. Plastino).
[1] Current address Laboratoire de physique de l'Ecole Normale Supérieure, ENS, Université PSL, CNRS, Sorbonne Université, Université de Paris, 75005 Paris, France.

https://doi.org/10.1016/j.ydbio.2021.12.013
Received 9 July 2021; Received in revised form 16 December 2021; Accepted 23 December 2021
Available online 28 December 2021

an asymmetric first division giving rise to a large anterior cell (AB) and a small posterior cell (P1), although the asymmetry is in some cases very subtle (Valfort et al., 2018), ii) an asynchrony of division between AB and P1 with AB being either first or second depending on species, iii) an asymmetric division of P1 whereas AB divides symmetrically (Delattre and Goehring, 2021).

Although the sperm centrosome is key in symmetry breaking in *C. elegans*, other species have been found to polarize independently of sperm, either because there is no sperm, as in parthenogenetic species, or because sperm is not the polarity cue (Goldstein et al., 1998; Lahl et al., 2006). What acts as the polarity cue and how symmetry is broken in these cases remains an open question, one which we address in this study using the parthenogenetic nematode *Diploscapter pachys*. Within the Rhabditidae family, the *Diploscapter* genus is the closest to the *Caenorhabditis* genus, to which the sexual species *C. elegans* belongs (Fradin et al., 2017). By a combination of live embryo imaging and dynamics analysis, cytoskeleton fixed staining at different stages and perturbing centrifugation experiments, we observe that, while many features of the asymmetric division process are conserved between *D. pachys* and *C. elegans*, the timing of polarity establishment and the correlation of the posterior pole with the location of the meiotic spindle are unique to *D. pachys*.

2. Materials and methods

2.1. Worm cultivation

Diploscapter pachys strain PF1309 was obtained from Hélène Fradin (Fradin et al., 2017). *Caenorhabditis elegans* strain N2 was from the Caenorhabditis Genetics Center. Strains were cultured at 20°C on 2.5% agar standard NGM plates for *C. elegans* worms and 5% NGM plates for *D. pachys* worms in order to reduce plate contamination and burrowing. Plates were seeded with the OP50 strain of *Escherichia coli* as a food source.

2.2. DIC microscopy

Gravid adults were cut in a watch glass in M9 buffer and embryos were transferred to a 2% Noble agarose pad. Embryos were imaged during asymmetric cell division by DIC microscopy. For time-lapse acquisitions the time between frames was 10 s. Long-term time-lapse imaging of egg hatching was acquired at an interval of 10 s for capturing first cell division, 30 s interval from 2-cell stage until 5 h after cleavage and 3-min interval for the remainder of the movie. To image embryos *in utero*, gravid worms were washed in water and then transferred to a 4.5% Noble agarose pad in 6 μL of M9 buffer containing 0.03% levamisole to immobilize the worms. The time interval for image acquisition was 10 s.

2.3. Centrifugation of embryos

Gravid adults were washed in 50% M9 and then dissected in 50% M9 on freshly coated poly-L-lysine slides (2.5 mg/mL, Sigma-Aldrich P1524). Embryos were aligned with their anterior/posterior (AP) axis parallel to the long axis of the microscope slide using an eyelash pick as they floated down to the slide surface. Slides were then placed in a 50 mL Falcon tube filled with 50% M9 and centrifuged in a Heraeus Biofuge at 2576×*g* (4000 rpm) for 15 min. The slide was then removed from the tube, and excess liquid around the embryos was removed before overlaying with a coverslip. Embryos were immediately imaged by DIC microscopy. A still image was taken of all properly aligned embryos, and then one embryo was filmed until division. Then a second still image was taken of the rest of the embryos to determine the final division positioning.

2.4. Image analysis

For nuclear positioning along the AP axis, the distance of the nucleus center from the future anterior pole, as well as the AP length, were measured in Image J (National Institutes of Health) every 10 min in the DIC movies. The percentage of nuclear position along AP axis was calculated by dividing the anterior to nucleus distance by the AP length. All averages are represented ± the standard deviation.

To quantify morphological dynamics of *D. pachys* embryos, we created training patches to train a 2D U-Net network to create masks from time lapse DIC movies (Ronneberger et al., 2015). We used an incremental learning approach where we applied the model prediction to unseen movies and used a Napari correction tool to manually correct each frame to create more training data for re-training the network. This version of the program was then applied to all raw movies to produce masks. The Logical XOR function of Metamorph (Molecular Devices) was applied to the mask stacks to highlight areas where embryo contours did not match.

2.5. Phalloidin staining of F-actin and imaging

The protocol was a combination of (Munro et al., 2004) and personal communication (François Robin, Institut de Biologie Paris Seine). Briefly gravid worms were washed in M9, dissected on a freshly coated poly-L-lysine slide, and incubated between 0 and 50 min depending on what age embryos were desired. A fixing solution containing 60 mM PIPES, 10 mM EGTA, 25 mM HEPES, 1 mM MgCl2, 0.1 mg/mL lysolecithin (Sigma-Aldrich 62962), 100 mM glucose, 3% paraformaldehyde and 0.2% glutaraldehyde was then added and incubated for 15 min. Slides were washed three times with PBS and then incubated overnight at 4°C in a 0.66 μM phalloidin Alexa Fluor 488 (Invitrogen 10125092) in PBS. Slides were gently washed with PBS and incubated for 2 h in PBS + Hoechst (0.5 μg/mL, Fisher Scientific H1399) at room temperature. Samples were washed again in PBS, and then sealed in a drop of Aqua-Poly/Mount (Polysciences, 18606) and viewed with a Roper/Zeiss upright spinning disk confocal microscope, equipped with a CoolSnap HQ2 camera and a 100x/1.46 OIL DIC ALPHA PL APO (UV) VIS-IR objective and controlled by Metamorph. Z-stack acquisition was obtained at a 0.3 μm step size. Images were processed with Metamorph and ImageJ. Linescans were obtained in Metamorph using a 3 μm line width in average mode drawn along the AP axis of the embryo, and background was subtracted.

2.6. Tubulin staining and imaging

Embryos were freeze-cracked following protocols established for *C. elegans* and other species (Riche et al., 2013). Briefly, gravid females were dissected on poly-L-lysine coated slides and flattened between slide and coverslip before being rapidly frozen on aluminum blocks. After cracking of the coverslip, slides were immersed in −20°C methanol for at least 5 min and later processed for staining. Staining was performed for 45 min in a mouse anti-tubulin antibody DM1a (Sigma-Aldrich) diluted 1:200, followed by 45 min in a secondary donkey anti-mouse antibody DyLight 488 (Jackson Immunoresearch) diluted 1:1000. Slides were then incubated for 5 min in 1 μg/ml Hoechst 33342 (Sigma-Aldrich). Images were acquired on Zeiss LSM710 confocal microscope with a 63x oil immersion objective. Images were processed with Metamorph and ImageJ.

3. RESULTS/DISCUSSION

3.1. Evidence of symmetry breaking in the one-cell embryo of D. pachys

D. pachys carries a single chromosome pair, and oocytes appear to skip meiosis I and undergo a single meiosis II-type nuclear division to separate sister chromatids, forming a polar body and a diploid embryo, which develops without fertilization (Fradin et al., 2017).

Most embryos dissected from gravid *D. pachys* females were at the one-cell stage, meaning that they had not yet undergone their first mitotic division. 80% were post-meiotic as evidenced by a clearly

delimited round shape of the nucleus (n = 34/43) while the remainder were just before or undergoing meiotic division. Most post-meiotic embryos took about 50 min to proceed to cleavage, passing through four recognizable stages in DIC microscopy: membrane ruffling, membrane smoothening, cleavage start and scission (Fig. 1A and Supplementary Movie 1). Ruffling was the longest stage, lasting 20–45 min depending on the specimen. About 15 min before the onset of cytokinesis, recognizable as membrane invagination, and about 5 min before nuclear envelope breakdown (NEBD), membrane ruffling abated and the embryo contour became smooth. From the start to finish of cleavage took about 5 min (Fig. 1A). As compared to *C. elegans*, the overall impression obtained from these films, which will be detailed more in the following, was that *D. pachys* embryos displayed more membrane activity in general than *C. elegans*, but that the asymmetric smoothening of one pole was lacking in *D. pachys*, there was no identifiable pseudocleavage furrow and cytoplasmic flows were chaotic. In addition there were no typical/reproducible spindle oscillations or spindle movements during anaphase, unlike *C. elegans*, but similar to other non-*Caenorhabditis* species (Valfort et al., 2018).

Supplementary video related to this article can be found at https://doi.org/10.1016/j.ydbio.2021.12.013

D. pachys embryos were also able to hatch between slide and coverslip, displaying recognizable stages as compared to *C. elegans*, but taking around 38 h to hatch from the time of cleavage initiation of the first cell division, as opposed to 9 h for *C. elegans* (Supplementary Fig. S1A and Supplementary Movie 2). As previously reported for a close parthenogenetic relative *Diploscapter coronatus* (Lahl et al., 2009), at the 2-cell stage of *D. pachys* embryos, one blastomere was slightly smaller than the other, and the smaller cell went on to divide before the other in an asymmetric manner, revealing that the embryo was polarized. By analogy with *C. elegans* and other nematodes, this cell was thus considered the posterior cell P1. In *D. pachys*, as in other members of the *Diploscapter* genus, the mitotic spindle in both AB and P1 was oriented along the longitudinal axis of the embryo (Goldstein, 2001; Lahl et al., 2009) (Supplementary Fig. S1A). Observing females that retained their embryos for longer in the uterus and/or examining egg-laying of anesthetized females, we followed cell division and confirmed, like for *D. coronatus* (Lahl et al., 2006), that there was no correlation between oocyte orientation in the uterus and the location of the posterior cell (N = 11: six embryos had their posterior pole adjacent to the vulva and five had their anterior pole towards the vulva). All of this information together indicated that the *D. pachys* embryo first cell division was asymmetric in the absence of a uterine cue and despite the lack of a paternal contribution.

Supplementary video related to this article can be found at https://doi.org/10.1016/j.ydbio.2021.12.013

More in detail we found that at the start of filming, the position of the maternal nucleus was variable although it was often positioned in the future posterior half of the embryo. Without exception by the end of smoothening, the nucleus had traveled to the part of the embryo that would become the posterior pole, and positioned itself at 54 ± 3% (N = 43) of the total length of the embryo (where 0% is the anterior pole and 100% is the posterior pole) by the beginning of cleavage (Fig. 1B). Indeed outlier embryos in both the anterior and posterior directions showed the most dramatic movements toward the 54% mark just before and during the smoothening period, and ended up dividing asymmetrically like the others (Fig. 1B). This result showed a strict correlation between the position of the post-meiotic nucleus and the position of the posterior pole.

3.2. The posterior pole is not determined by the position of the post-meiotic nucleus

The question was then if this were causal: did the position of the nucleus define the posterior pole? To test this, we perturbed nuclear position by centrifugation of live embryos adhered to microscope slides in order to shift the nucleus to one side of the embryo and see if that pole became the posterior. Only embryos that were positioned with their long anterior-posterior (AP) axis parallel to the centrifugation force were considered. Due to the duration of the mounting and centrifugation treatment, most (92%) of the embryos were post-meiotic after centrifugation. These post-meiotic nuclei were, in the majority of cases, found at the pole opposite to the centrifugal force (29/33 embryos) (Fig. 1C). This was unanticipated, but indicated that most nuclei were less dense than other contents of the embryo, and in the following, we considered only this larger population of 29 embryos. Using these 29 embryos, we evaluated which end of the embryo became the posterior pole, based on size and by P1 cell division (dividing before AB): 17 were filmed post-centrifugation, and the remaining 12 were evaluated by still images taken just after centrifugation and then again upon cell division. In 14/29 embryos (nine movies and five still images), the posterior of the cell was found at the pole where the nucleus was initially observed post-centrifugation (Fig. 1C and Supplementary Movie 3). However, in the remaining 15/29 embryos (eight movies and seven still images), P1 was observed at the opposite pole from where the nucleus was initially observed post-centrifugation (Fig. 1D Supplementary Movie 4). Tracking nuclear position over time for the filmed embryos revealed that most centrifuged embryos shifted their nuclei to establish an off-centered division plane, with a smaller posterior cell, but there were some exceptions, unlike for non-centrifuged embryos (Fig. 1E and F). In particular several of the embryos whose posterior pole was opposite to the pole where the nucleus was found post-centrifugation no longer displayed a smaller posterior cell, although the posterior cell still divided before AB (Fig. 1F). All together these results suggested that polarity of the embryo was set upstream of post-meiotic nuclear positioning since the initial location of the nucleus after centrifugation did not correlate with the future posterior pole of the embryo. Early pole definition also explained the behavior of outliers with anteriorly-positioned nuclei in non-centrifuged embryos, whose nuclei migrated directionally toward the future posterior pole (Fig. 1B).

Supplementary video related to this article can be found at https://doi.org/10.1016/j.ydbio.2021.12.013

3.3. Cortical ruffling and actin cytoskeleton are not polarized in post-meiotic embryos

This result echoed what was known for the *C. elegans* embryo where polarity is established well before nuclear positioning for division. As discussed in the introduction, polarization is typified by dissimilar cortical dynamics at the two embryo poles, visible by live DIC microscopy as enhanced ruffling at the anterior pole during pronuclear meeting and centering, as well as by live or fixed actin cytoskeleton labelling, which shows enrichment of actin and myosin at the anterior pole (Munro et al., 2004; Reymann et al., 2016; Strome, 1986). We therefore looked for some indication that the *D. pachys* embryo had polarized cortical activity by first assessing DIC movies. We created masks via machine learning to automatically detect embryo contours over time, and compared them with an either/or function where white pixels indicated presence of signal in only one of two consecutive frames being compared (Fig. 2A and Supplementary Movie 5 and 6). In this analysis the width of the margin of white pixels gave a visualization of contour changes, with a thicker band indicating more variability and thus more cortical activity. Breaking the time-lapse down into early ruffling, late ruffling and smoothening phases, we observed a decrease in band thickness over time as smoothening occurred (going from left to right in Fig. 2B), but there were no obvious differences in margin thickness when comparing the future posterior and anterior poles. Indeed, this was true for a whole population of embryos (N = 25) where plotting margin thickness at the anterior pole versus thickness at the posterior pole during the ruffling phase gave a linear relation with a slope of one (Fig. 2B). So, although there was considerable variability in the contours explored by different embryos (margin thicknesses range from one to seven μm), the activity at the posterior and anterior poles was indistinguishable. If the anterior were more active, for example, the line would have had a slope greater than one.

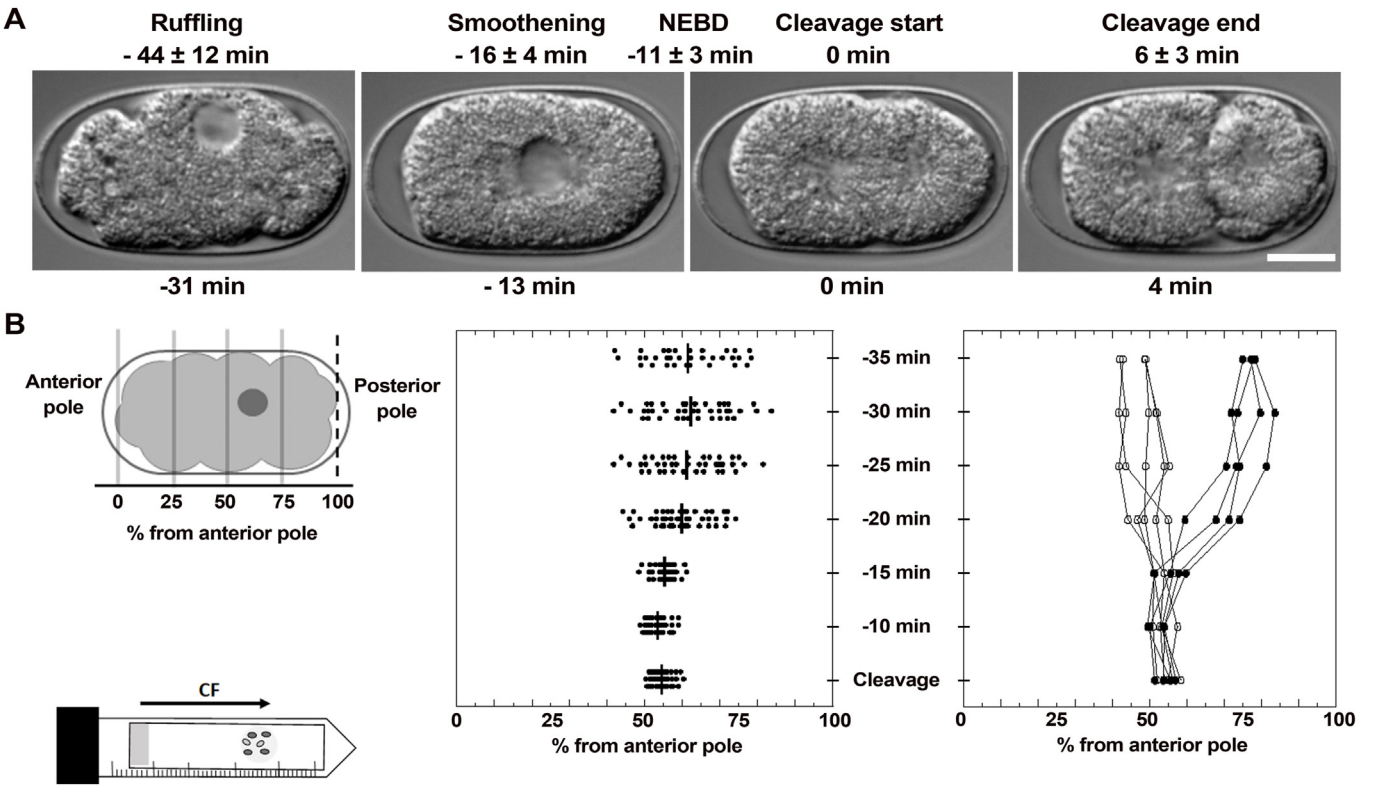

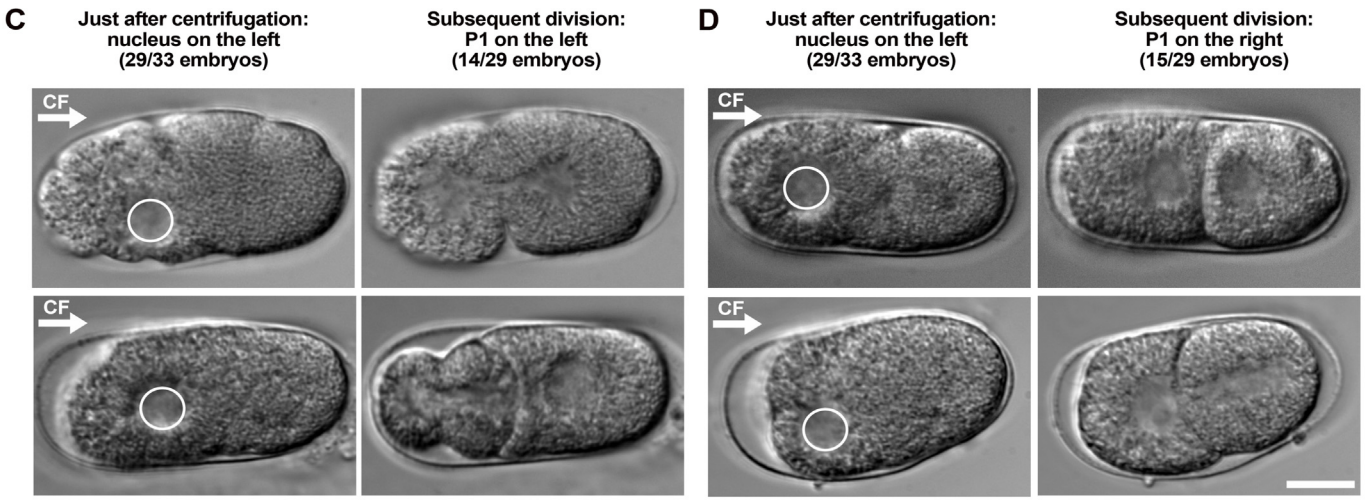

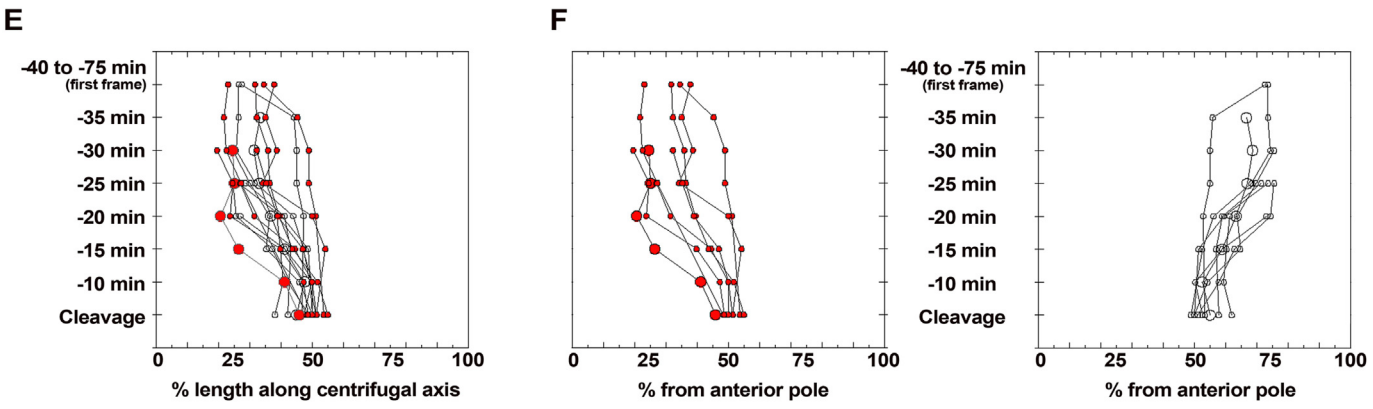

(caption on next page)

Supplementary video related to this article can be found at https://doi.org/10.1016/j.ydbio.2021.12.013

We next sought to observe a difference in actin cytoskeleton between the embryo poles in *D. pachys*. Due to a lack of transgenic techniques in *D. pachys*, we attempted to apply vital dyes by different means, including feeding loaded liposomes (Flavel et al., 2018) and *perm-1* RNAi (Fradin et al., 2017) without success. We therefore turned to phalloidin staining of F-actin in fixed embryos, using DNA labeling to stage the embryos. Since for *C. elegans,* actin polarization is only evident post-meiotically and then diminishes around cleavage, we initially focused on *D. pachys* embryos that displayed a clear polar body extrusion indicating that meiosis had already taken place. For post-meiotic *D. pachys* embryos, we observed no consistent actin asymmetry at early and late prophase and metaphase stages (N = 38), whereas in all the *C. elegans* controls (N = 36 for early and late prophase and metaphase stages), processed for imaging via the same method as used for *D. pachys*, there was clear enrichment of actin at the future anterior pole (Fig. 2C and D). Neither species showed much actin asymmetry in the two-cell stage (Fig. 2C and D). The fact that the post-meiotic *D. pachys* embryo had a nonpolarized actin cytoskeleton resonated with the homogeneity of cortical activity quantified with live embryos (Fig. 2A and B). However this lack of polarity was not in keeping with our centrifugation results, which indicated that the nucleus had a clear preference for one pole of the embryo post-meiotically. This led us to the hypothesis that polarity in *D. pachys* was generated early, during or before meiosis in the oocyte.

3.4. The meiotic spindle correlates with the future posterior pole in D. pachys oocytes

In *C. elegans*, the meiotic spindle is usually at the anterior pole, but the relationship is not causal. The real polarity signal is released by the sperm centrosome, and the posterior pole is therefore defined by sperm centrosome location (Bienkowska and Cowan, 2012; Goldstein and Hird, 1996; Kimura and Kimura, 2020). However in mutant cases in *C. elegans* where there is a persistent meiotic spindle, it has been shown that signaling from the spindle can establish polarity and define the posterior pole, so this role is not unique to the sperm centrosome (Wallenfang and Seydoux, 2000). Given this context we looked for a role of the meiotic spindle in symmetry breaking in *D. pachys* by examining the 20% of our DIC movies (nine embryos) that began early enough to include meiosis. The meiotic spindle was invariably found on the lateral side of the oocyte, not at the pole of the cell in contrast to *C. elegans*. Nevertheless in all nine cases, the meiotic spindle was found slightly off-centered along the AP axis, and was always closer to the future posterior pole (Fig. 3A). In a previous study on a sister parthenogenetic species, *Diplosapter coronatus*, the authors came to the conclusion that there was no correlation between the polar body and the posterior pole (Lahl et al., 2006), however we were looking at meiotic spindle formation as opposed to polar bodies whose position can drift once they are formed. Our result suggested a link between the location of the meiotic spindle and the future posterior pole in the *D. pachys* oocyte.

3.5. D. pachys oocytes display a meiotic microtubule aster and actin asymmetry

Given the previously-mentioned result that microtubules emanating from persistent meiotic spindles in mutant *C. elegans* embryos can trigger embryo polarity (Wallenfang and Seydoux, 2000), we set out to assess microtubule structures in the *D. pachys* oocyte that could potentially act as polarizing cues. We stained oocytes for microtubules, and found that, before meiotic spindle formation, oocytes exhibited a large microtubule aster between the chromosomes, a structure not observed in *C. elegans* (Fig. 3B). During meiotic division, we observed a cage of microtubules around the chromosomes resembling a *C. elegans* meiotic spindle, but with unusual microtubule extensions reaching out on the side directed toward the cell border (Fig. 3B). Either one of these structures could potentially communicate with the cortex during meiotic division, delivering an unknown signal/triggering an unknown process and setting the polarity of the embryo.

To see if there was any manifestation of polarity establishment in the actin cytoskeleton at this stage, we phalloidin stained pre-meiotic embryos, before polar body formation as evaluated by DNA staining. Of a total of 16 pre-meiotic embryos, we observed nine that exhibited a slightly polarized actin cytoskeleton with one hemisphere being richer in actin than the other (Fig. 3C). In seven cases out of nine, the DNA was in the actin-rich pole of the embryo. Assuming that the location of pre-meiotic DNA corresponded to the site of the future meiotic spindle, and given the correlation of the meiotic spindle with the posterior pole, we concluded from this that actin enrichment was posterior, unlike what is observed in *C. elegans*. Also, unlike *C. elegans*, actin polarization was weaker, more fleeting and less consistent in the *D. pachys* embryo so it was difficult to conclude. However, in this context, it is important to note that even for *C. elegans*, only certain stages of the first cell division exhibit clear actin asymmetry by phalloidin staining, and that even when asymmetry fades upon cytokinesis, the embryo retains its polarity.

3.6. Asymmetry is not induced by the oocyte nucleus before meiosis in D. pachys

Despite these results indicating an asymmetry at meiosis, we could not rule out the possibility that asymmetry was established even earlier by the oocyte nucleus. Indeed in *C. elegans* the −1 oocyte nucleus undergoes a movement proximally, away from the spermatheca, implying some polarity in the oocyte (McCarter et al., 1999; Reich et al., 2019;

Fig. 1. Nuclear positioning during the first cell division of *D. pachys* embryos. A. DIC still images of asymmetric cell division, showing cortical ruffling followed by smoothening and cleavage. The different phases are labeled with the average times recorded (N = 43), and the exact times for this embryo are given below the images. Nuclear membrane breakdown (NEBD) average time is also indicated. **B.** Cartoon depicting how the position of the nucleus (dark grey sphere) is measured as a percentage of the AP axis from the future anterior pole (0% on x-axis). Left graph: scatter plot of quantification of nuclear position over time, expressed as % from the anterior pole with time normalized to time of start of cleavage. Right plot: outlier embryos that have nuclei located at either ≤50% (open circles) or >70% (closed circles) replotted separately to see how they reposition over the course of cell division. All embryos end with cleavage at about 54% from the posterior pole. (N = 43). **C. and D.** Centrifugation experiment. Cartoon shows how embryos adhering to a microscope slide are centrifuged in a Falcon tube in a swinging bucket. Centrifugation force is indicated with an arrow labeled CF, and is directed toward the right in all images. Only embryos with their long axis parallel to the centrifugation force (dark grey embryos in the cartoon) are analyzed. Dividing *D. pachys* embryos are centrifuged and observed immediately, and then again during/after the first division. Nuclei are found predominantly on the opposite side as compared to the centrifugal force in the initial observations. **C.** Embryos where the nucleus did not reposition, and where eventually the posterior cell formed as shown by size (top panels) and P1 cell division (bottom panels). **D.** Embryos where the nuclei migrated to the opposite side of the embryo before division, and the posterior cell formed as shown by size (top panels) and the beginning of P1 cell division (bottom panels). **E., F.** Nuclei tracking in embryos post-centrifugation. Red filled symbols indicate embryos whose posterior pole was opposite the initial position of the nuclei after centrifugation. Open symbols indicate embryos whose posterior pole and post-centrifugation nuclear position coincided. Larger symbols correspond to the embryos shown in **C. and D.** (bottom panels) and to Supplementary Movies 3 and 4. **E.** shows all filmed nuclei plotted in relation to the centrifugal axis, while **F.** shows the traditional representation in relation to % from the anterior pole, with the two types of embryos represented in separate graphs for clarity. Bars 10 μm.

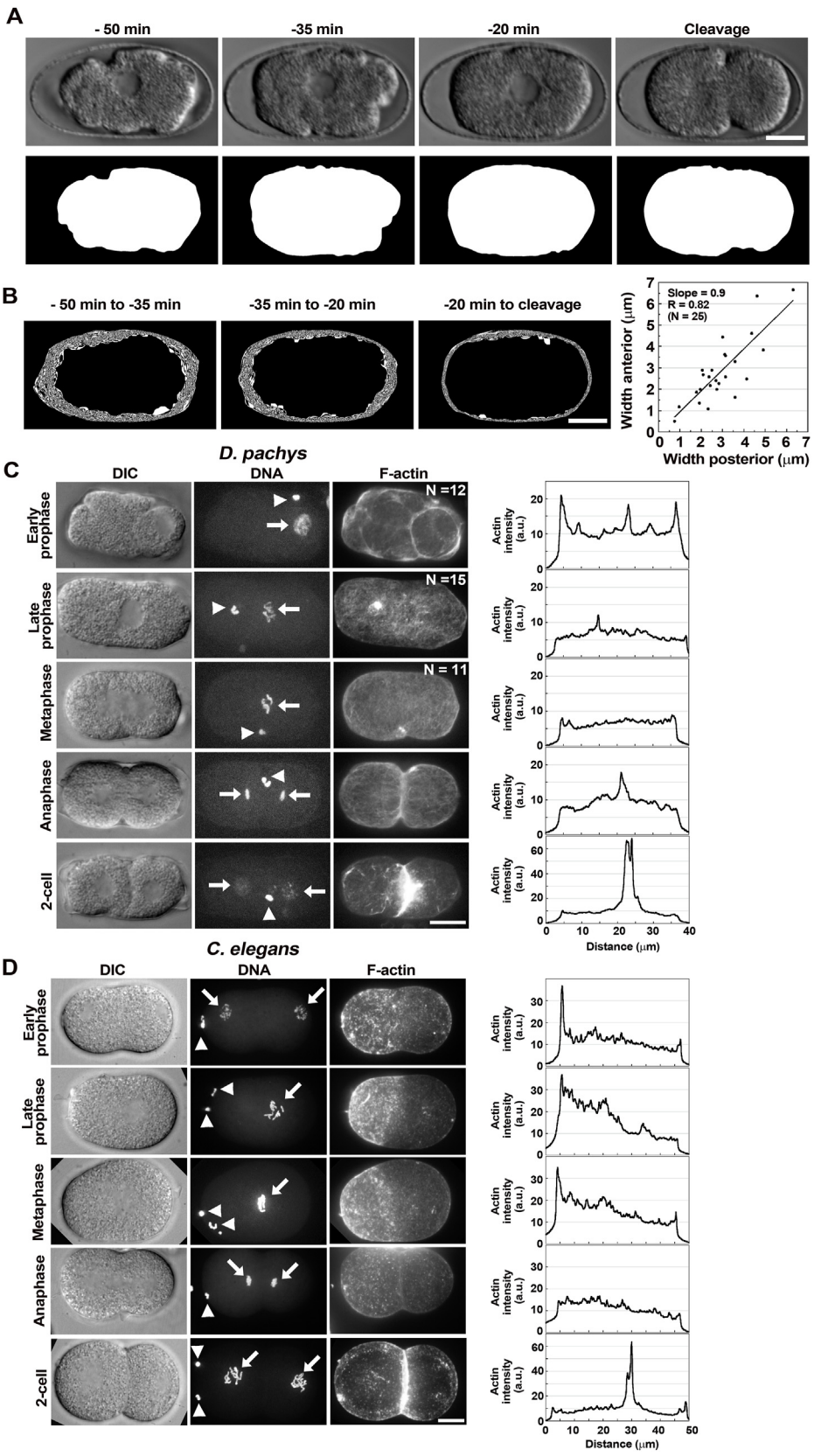

Fig. 2. Cortical ruffling and actin cytoskeleton in post-meiotic *D. pachys* embryos. A. DIC images of different stages (top) and the corresponding masks that are used to calculate cortical deformations (bottom). **B.** Movies were divided into early and late ruffling and smoothening stages, and embryo contours obtained from the masks were analyzed with an either/or function. In this analysis the white margins indicate unshared pixels between frames, and are a reflection of contour deformation. The graph plots the width of the anterior versus the posterior deformation as measured along the AP axis up to the smoothening phase. The data is roughly linear with a slope of 1 meaning that the activity of the poles is not significantly different. (N = 25). **C.** Spinning disc images of fixed staining of F-actin (phalloidin Alexa-488) and DNA (Hoechst) of the *D. pachys* embryo at different stages of cell division: earlier stages at the top (starting with early prophase) to late stages at the bottom (ending with two-cell embryo). DNA images are the maximum intensity projection of the embryo stack so as to see both the nucleus (arrows) and the polar bodies (arrowheads), while F-actin is a sum projection of the stack. The N values reported on the actin sum projections are the number of embryos observed at each stage. On the right are accompanying linescans for each actin image. Peaks for actin intensity are homogeneous along the AP axis of all embryos indicating no actin asymmetry at any stage. **D.** The same as **C.**, but with *C. elegans* embryos for comparison. Clear actin asymmetry is visible at early stages in the images and the linescans as per other published works. Bars 10 μm.

Rutledge et al., 2001). To test whether this was occurring in *D. pachys*, we examined oocytes pre-meiosis in anesthetized worms. Nuclei were centered and immobile in −1 oocytes (Fig. 3D and Supplementary Movie 7). In the dozen oocytes at the −1 position examined, we never observed directed movements of the oocyte nucleus or a reproducible correlation with one of the oocyte borders, although upon ovulation (passage via a constriction into the vestigial spermatheca), the embryo was much deformed and the nucleus sometimes approached an embryo edge.

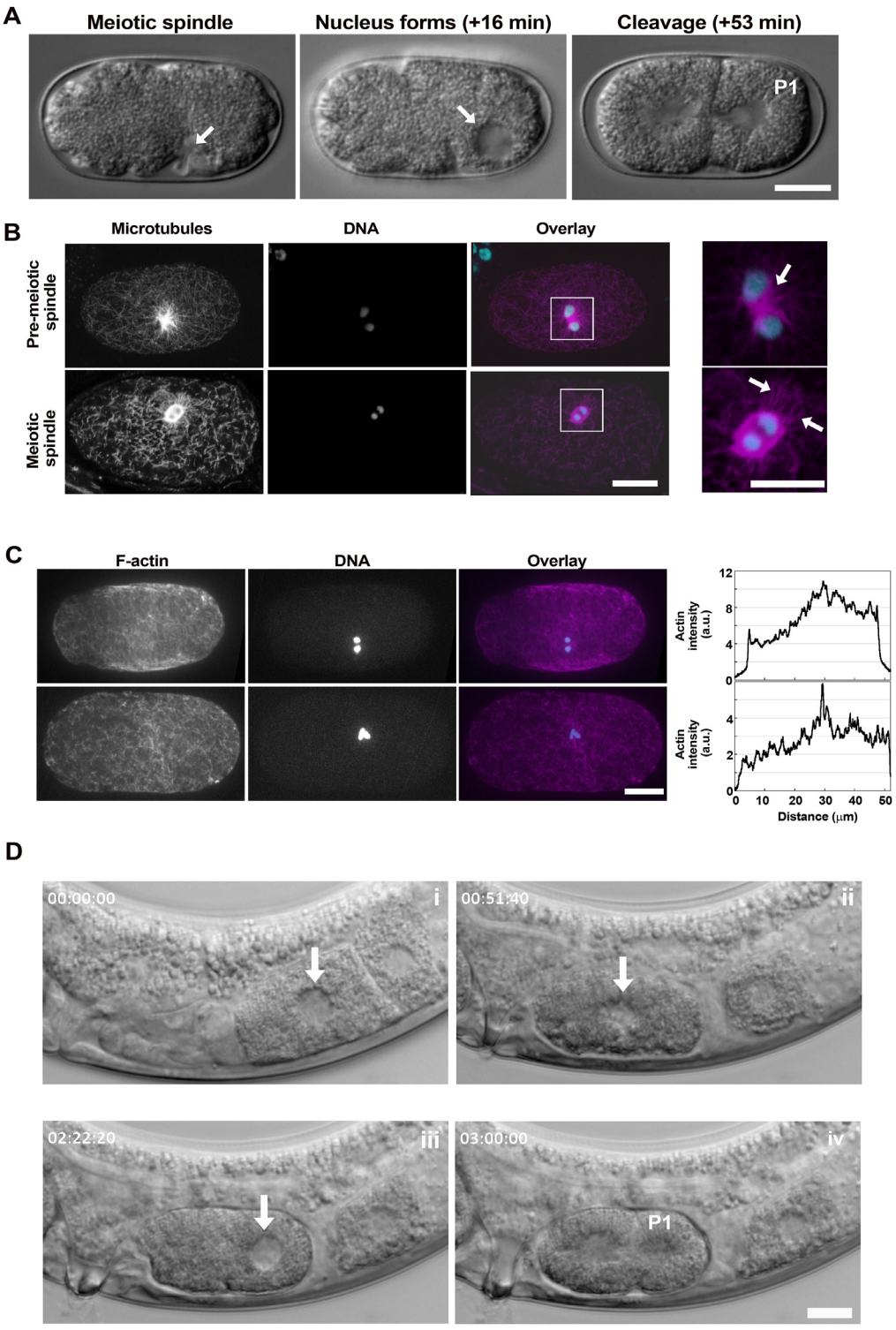

Fig. 3. Meiotic spindle, microtubules and actin before completion of meiosis in *D. pachys* embryos and nuclear position in oocytes. A. DIC images of a typical meiotic spindle localization and subsequent cleavage. Meiotic spindles are always lateral and closer to the side of the embryo that becomes the posterior pole. Meiotic spindle and nucleus are marked with white arrows and P1 is labeled. **B.** Confocal images of immunofluorescence visualization of microtubules on the pre-meiotic DNA and the nascent meiotic spindle. Maximum intensity projections of the embryo stack in microtubule and DNA channels and overlays. Zooms of the overlays are shown on the right. Arrows indicate microtubule asters and extensions. As an aside, in this zoom of DNA staining, the fact that the homologous chromosomes of the single pair do not synapse and recombine is evident, and two univalents are in fact observed at the onset of meiotic division. **C.** Spinning disc images of F-actin in pre-meiotic embryos. DNA images are the maximum intensity projection of the embryo stack, while F-actin is a sum projection of the stack. A slight asymmetry is evident by eye and is visible in the linescans. The actin-rich pole is often where the DNA is found and where presumably meiosis will take/is taking place. As evident in the images, pre-meiotic embryos were of more variable size and consistently larger than later-stage fixed embryos, perhaps due to the immature eggshell and osmotic swelling before fixation. **D.** Nuclear positioning in oocytes before ovulation. As indicated by the arrows, the nucleus is centered in the oocyte just before ovulation, but slightly offset as meiosis begins, post-ovulation (panels i and ii). When the nucleus reforms after meiosis (panel iii), it is asymmetrically positioned and closer to the posterior pole, which upon division gives the smaller P1 cell (panel iv). Bars 10 μm. Bars on zooms 5 μm.

Meiosis subsequently occurred wherever the nucleus ended up after the drastic deformations of ovulation, and that then became the posterior pole (Supplementary Movie 7).

Supplementary video related to this article can be found at https://doi.org/10.1016/j.ydbio.2021.12.013

4. Conclusion

Putting all the data together, we conclude that the *D. pachys* embryo is polarized very early in development, at the unique meiotic division of the oocyte. The data is consistent with the location of the meiotic spindle defining the posterior pole. The invariably lateral position of the meiotic spindle would seem incompatible with hemispheric polarity. However in *C. elegans* it has been shown that when polarity emerges off-axis, re-alignment of PAR domains along the long axis can occur (Gessele et al., 2020; Schenk et al., 2010). A similar corrective mechanism could be operational in the *D. pachys* case. The question remains as to the nature of the polarity cue. The microtubule structures observed at meiosis could contribute to the symmetry breaking event. In *C. elegans* there are multiple levels of redundancy to ensure polarization via the sperm (Delattre and Goehring, 2021). In particular PLK-1 and AIR-1 have been shown in *C. elegans* to prevent precocious polarization in oocytes caused by cryptic cues coming from the female pronucleus and the meiotic spindle (Reich et al., 2019) or even from curvature (Klinkert et al., 2019). We hypothesize that this inhibition is not at work in *D. pachys*, leading to very early polarization.

As concerns PAR proteins in the *D. pachys* embryo, it has been shown in a sister *Diploscapter* species that PAR-1 is symmetrically distributed in the one-cell embryo just before division (Brauchle et al., 2009) seemingly shedding doubt on a role for the PAR network in polarity of the *D. pachys* embryo. However it is of note that there are cases in *C. elegans* where PAR-1 is uniform, but normal asymmetric division occurs nonetheless (Folkmann and Seydoux, 2019). Furthermore, it is entirely possible the PAR paradigm conceived for *C. elegans* is not the whole story in other species, and that additional PAR regulatory proteins or altogether different polarity proteins play a role (Basham and Rose, 1999; Brauchle et al., 2009; Morton et al., 2012).

To conclude although many open questions remain, what is clear from this study is that already at meiosis, there is a difference between the poles of the *D. pachys* oocyte, which drives polarity of the embryo. *Diploscapter* is the only genus known to date within the Rhabditidae family, which includes *C. elegans*, to polarize independently of a sperm centrosome-derived cue. It is therefore of particular importance to further study self-organization and symmetry breaking in this species in order to bring to light alternative/redundant pathways for symmetry breaking that are obscured in *C. elegans*, where the sperm centrosome mechanism is dominant.

Funding information

J.P. acknowledges financial support for this work from the Fondation pour la Recherche Médicale (Grant DEQ20120323737) and the Fondation ARC (Grant PJA 20151203487 and Grant PJA 20191209604). This work also received support under the program "Investissements d'Avenir" launched by the French Government and implemented by ANR (ANR-10-LABX-0038 and ANR-10-IDEX-0001-02 PSL). M.D. received financial support from the CNRS, from the ANR (ANR-19-CE02-0012) and from CEFIPRA (62T5-1). D.S.E. was funded by the European Union's Horizon 2020 research and innovation programme under the Marie Skłodowska-Curie grant agreement No 666003, and by the Fondation pour la Recherche Médicale (Grant FDT202001010816).

Declaration of interests

The authors declare that they have no conflicts of interest with the contents of this article.

Acknowledgments

We warmly acknowledge Olivier Renaud and Olivier Leroy of the Cell and Tissue Imaging Platform (member of France BioImaging, ANR-10-INBS-04) of the Genetics and Developmental Biology Department (UMR3215/U934) of Institut Curie for help with light microscopy. We also thank François Robin (Institut de Biologie Paris Seine) for help with phalloidin staining, Jean-Léon Maître (Institut Curie) for expert advice and Varun Kapoor (Institut Curie) for discussions on image analysis.

Appendix A. Supplementary data

Supplementary data to this article can be found online at https://doi.org/10.1016/j.ydbio.2021.12.013.

References

Basham, S.E., Rose, L.S., 1999. Mutations in ooc-5 and ooc-3 disrupt oocyte formation and the reestablishment of asymmetric PAR protein localization in two-cell *Caenorhabditis elegans* embryos. Dev. Biol. 215, 253–263.
Bienkowska, D., Cowan, C.R., 2012. Centrosomes can initiate a polarity axis from any position within one-cell *C. elegans* embryos. Curr. Biol. 22, 583–589.
Brauchle, M., Kiontke, K., MacMenamin, P., Fitch, D.H.A., Piano, F., 2009. Evolution of early embryogenesis in rhabditid nematodes. Dev. Biol. 335, 253–262.
Delattre, M., Goehring, N.W., 2021. The first steps in the life of a worm: themes and variations in asymmetric division in *C. elegans* and other nematodes. Curr. Top. Dev. Biol. 144, 269–308.
Flavel, M.R., Mechler, A., Shahmiri, M., Mathews, E.R., Francks, A.E., Chen, W., Zanker, D., Xian, B., Gao, S., Luo, J., Tegegne, S., Doneski, C., Jois, M., 2018. Growth of *Caenorhabditis elegans* in defined media is dependent on presence of particulate matter. G3 8, 567–575.
Folkmann, A.W., Seydoux, G., 2019. Spatial regulation of the polarity kinase PAR-1 by parallel inhibitory mechanisms. Development 146, dev171116.
Fradin, H., Kiontke, K., Zegar, C., Gutwein, M., Lucas, J., Kovtun, M., Corcoran, D.L., Baugh, L.R., Fitch, D.H.A., Piano, F., Gunsalus, K.C., 2017. Genome architecture and evolution of a unichromosomal asexual nematode. Curr. Biol. 27, 2928–2939.
Gan, W.J., Motegi, F., 2021. Mechanochemical control of symmetry breaking in the *Caenorhabditis elegans* zygote. Front. Cell Dev. Biol. 8, 619869.
Gessele, R., Halatek, J., Würthner, L., Frey, E., 2020. Geometric cues stabilise long-axis polarisation of PAR protein patterns in *C. elegans*. Nat. Commun. 11, 539.
Goldstein, B., 2001. On the evolution of early development in the Nematoda. Phil. Trans. Roy. Soc. Lond. B 356, 1521–1531.
Goldstein, B., Frisse, L.M., Thomas, W.K., 1998. Embryonic axis specification in nematodes: evolution of the first step in development. Curr. Biol. 8, 157–160.
Goldstein, B., Hird, S.N., 1996. Specification of the anteroposterior axis in *Caenorhabditis elegans*. Development 122, 1467–1474.
Gönczy, P., 2008. Mechanisms of asymmetric cell division: flies and worms pave the way. Nat. Rev. Mol. Cell Biol. 9, 355–366.
Hird, S.N., White, J.G., 1993. Cortical and cytoplasmic flow polarity in early embryonic cells of *Caenorhabditis elegans*. J. Cell Biol. 121, 1343–1355.
Kapoor, S., Kotak, S., 2019. Centrosome Aurora A regulates RhoGEF ECT-2 localisation and ensures a single PAR-2 polarity axis in C. elegans embryos. Development 146, dev174565.
Kimura, K., Kimura, A., 2020. Cytoplasmic streaming drifts the polarity cue and enables posteriorization of the *Caenorhabditis elegans* zygote at the side opposite of sperm entry. Mol. Biol. Cell 31, 1765–1773.
Klinkert, K., Levernier, N., Gross, P., Gentili, C., von Tobel, L., Pierron, M., Busso, C., Herrman, S., Grill, S.W., Kruse, K., Gönczy, P., 2019. Aurora A depletion reveals centrosome-independent polarization mechanism in. *Caenorhabditis elegans* eLife 8, e44552.
Knoblich, J.A., 2010. Asymmetric cell division: recent developments and their implications for tumour biology. Nat. Rev. Mol. Cell Biol. 11, 849–860.
Lahl, V., Sadler, B., Schierenberg, E., 2006. Egg development in parthenogenetic nematodes: variations in meiosis and axis formation. Int. J. Dev. Biol. 50, 393–398.
Lahl, V., Schulze, J., Schierenberg, E., 2009. Differences in embryonic pattern formation between *Caenorhabditis elegans* and its close parthenogenetic relative *Diploscapter coronatus*. Int. J. Dev. Biol. 53, 507–515.
McCarter, J., Bartlett, B., Dang, T., Schedl, T., 1999. On the control of oocyte meiotic maturation and ovulation in *Caenorhabditis elegans*. Dev. Biol. 205, 111–128.
Morton, D.G., Hoose, W.A., Kemphues, K.J., 2012. A genome-wide RNAi screen for enhancers of *par* mutants reveals new contributors to early embryonic polarity in *Caenorhabditis elegans*. Genetics 192, 929–942.
Munro, E., Nance, J., Priess, J.R., 2004. Cortical flows powered by asymmetrical contraction transport PAR proteins to establish and maintain anterior-posterior polarity in the early *C. elegans* embryo. Dev. Cell 7, 413–424.
Reich, J.D., Hubatsch, L., Illukkumbura, R., Peglion, F., Bland, T., Hirani, N., Goehring, N.W., 2019. Regulated activation of the PAR polarity network ensures a timely and specific response to spatial cues. Curr. Biol. 29, 1911–1923.
Reymann, A.-C., Staniscia, F., Erzberger, A., Salbreaux, G., Grill, S.W., 2016. Cortical flow aligns actin filaments to form a furrow. eLife 5, e17807.

Riche, S., Zouak, M., Argoul, F., Arneodo, A., Pecreaux, J., Delattre, M., 2013. Evolutionary comparisons reveal a positional switch for spindle pole oscillations in *Caenorhabditis embryos*. J. Cell Biol. 201, 653–662.

Ronneberger, O., Fischer, P., Brox, T., 2015. U-Net: convolutional networks for biomedicalImage segmentation. MICCAI 9351, 234–241.

Rose, L., Gönczy, P., 2014. Polarity establishment, asymmetric division and segregation of fate determinants in early *C. elegans* embryos. WormBook. https://doi.org/10.1895/wormbook.1891.1830.1892.

Rutledge, E., Bianchi, L., Christensen, M., Boehmer, C., Morrison, R., Broslat, A., Beld, A.M., George, A.L., Greenstein, D., Strange, K., 2001. CLH-3, a ClC-2 anion channel ortholog activated during meiotic maturation in C. elegans oocytes. Curr. Biol. 11, 161–170.

Schenk, C., Bringmann, H., Hyman, A.A., Cowan, C.R., 2010. Cortical domain correction repositions the polarity boundary to match the cytokinesis furrow in *C. elegans* embryos. Development 137, 1743–1753.

Schulze, J., Schierenberg, E., 2011. Evolution of embryonic development in nematodes. EvoDevo 2, 18.

Strome, S., 1986. Fluorescence visualization of the distribution of microfilaments in gonads and early embryos of the nematode *Caenorhabditis elegans*. J. Cell Biol. 103, 2241–2252.

Valfort, A.-C., Launay, C., Sémon, M., Delattre, M., 2018. Evolution of mitotic spindle behavior during the first asymmetric embryonic division of nematodes. PLoS Biol. 16, e2005099.

Wallenfang, M.R., Seydoux, G., 2000. Polarization of the anterior–posterior axis of *C. elegans* is a microtubule-directed process. Nature 408, 89–92.

Zhao, P., Teng, X., Tantirimudalige, S.N., Nishikawa, M., Wohland, T., Toyama, Y., Motegi, F., 2019. Aurora-A breaks symmetry in contractile actomyosin networks independently of its role in centrosome maturation. Dev. Cell 48, 631–645.